Colloid & Polymer Science Colloid & Polymer Sci 263:756–766 (1985)

Formation of rodlike micelles of dimethyloleylamine oxide in aqueous solutions: effects of addition of HCl and NaCl on the micelle size and the intermicellar interaction

T. Imae and S. Ikeda

Department of Chemistry, Faculty of Science, Nagoya University, Nagoya, Japan

Abstract: Angular dependence of light scattering has been measured for aqueous solutions of dimethyloleylamine oxide in the presence of HCl and NaCl. In micellar solutions more concentrated than 0.1×10^{-2} g cm^{-3}, rodlike micelles are dominantly formed, and their properties are strongly reflected in the characteristics of the solutions. The aggregation number, radius of gyration and even flexibility of the rodlike micelles increase with the addition of HCl as well as NaCl. The increase of HCl concentration up to 10^{-3} N makes the aggregation number of rodlike micelles as large as 58,000, when 0.01 M NaCl is present. The large micelle size would be stabilized by the dehydration of the amine oxide group and the hydrogen bonding between nonprotonated and protonated molecules in a micelle.

In aqueous solutions without HCl and NaCl or in their presence at very low concentrations, the light scattering is subject to the effects of both external and internal interferences. The effect of external interference can be separated from the effect of internal interference by applying the Zernike-Prins equation to the observed angular dependence of light scattering. Then the second virial coefficient and the pair interaction potential of rodlike micelles can be derived by means of certain approximate methods. The addition of HCl to 10^{-3} N makes both repulsive and attractive forces stronger and the resulting potential well deeper, but the addition of NaCl depresses such an effect of HCl considerably.

Key words: Light scattering, dimethyloleylamine oxide, rodlike micelle, wormlike chain, external interference.

Introduction

According to our light scattering studies [1, 2], dimethyloleylamine oxide, $CH_3(CH_2)_7CH = CH(CH_2)_8N(CH_3)_2O$, forms large rodlike micelles in water and in aqueous NaCl solutions, but it behaves rather anomalously in various respects. The molecular weight of rodlike micelles increases with increasing NaCl concentration, and their contour lengths are seven times longer in 0.05 M NaCl than in water. The large aggregation number is mainly caused by the strong cohesion between long hydrocarbon chains. The rodlike micelles behave as wormlike chains having a constant diameter of their cross-sections [2, 3], and their flexibility is chiefly determined by the strong hydration of amine oxide grops in solution. However, it is also dependent on the aggregation number or the contour length.

In aqueous solutions with zero or low NaCl concentrations, the effect of external interference was more dominant than that of internal interference, indicating strong intermicellar interaction [1]. The Zernike-Prins equation [4] has been applied for the observed angular dependence of light scattering to separate the two interference effects, and the Percus-Yevick or Hypernetted Chain equation in the theory of simple liquids [5] has been applied to derive the pair potential of interaction between the rodlike micelles.

In this work we measure light scattering from aqueous solutions of dimethyloleylamine oxide in the presence of HCl and NaCl. Since the amine oxide is a weak base having pK around 5–6, it is protonated in the presence of HCl and behaves as an electrolyte. Dimethyloleylamine oxide forms charged micelles in the presence of HCl, and micelles would be still predominantly rodlike, in spite of electrostatic repulsion. The size of rodlike micelles and their flexibility and mutual interaction may be affected by partial or total participation of the cationic form, i. e., dimethyloleyl-N-hydroxyammonium ion, $CH_3(CH_2)_7CH{=}CH(CH_2)_8N^+(CH_3)_2OH$, in place of the nonionic form.

Experimental

Materials

The sample of dimethyloleylamine oxide was the same as that previously used [1–3]. Special grade NaCl was ignited for two hours and stored in a desiccator until use. Water was redistilled from alkaline $KMnO_4$ solution. Solutions were prepared by diluting the stock solution of dimethyloleylamine oxide with aqueous NaCl and HCl solutions and kept overnight at room temperature before each measurement.

Measurements

The measurement of light scattering was performed on a Shimadzu Light Scattering Photometer PG-21 at 25 ± 0.05 °C. Unpolarized light of a mercury lamp at 436 nm was used. Details of measurement have already been described [1, 2]. The intensity of light scattering in the directions from 23 ° to 150 ° was measured.

The solvents and solutions were purified by filtering into a cylindrical cell under pressure through a Millipore filter GSWP, which had a pore size of 0.22 μm. The concentration of solutions after the filtration was determined from the optical density observed at the maximum wavelength of an ultraviolet absorption band, by referring to the calibration curve of the optical density for the concentration.

The refractive index increment was measured on a Shimadzu Differential Refractometer DR-3 at the wavelength of 436 nm of a mercury lamp at 25 ± 0.05 °C. The values of the specific refractive index increment were constant over the surfactant concentrations up to 0.3×10^{-2} g cm^{-3}, except for those in 0.05 M NaCl. In 0.05 M NaCl solutions, the specific refractive index increment was increased at higher surfactant concentrations, but the constant values were observed at low surfactant concentrations which covered the concentration range for light scattering measurements.

The pH of solutions was measured on an Iwaki Glass pH/ion Meter M-225 at room temperature (25 ± 1 °C).

Results

Light scattering at high NaCl concentrations

The reduced intensity of light scattering in the 90 ° direction, R_{90}, and its angular dissymmetry, $Z_{45} = R_{45}/R_{135}$, are shown in figure 1 as functions of surfactant concentration for 0.05 M NaCl solutions of dimethyloleylamine oxide in the presence of added HCl.

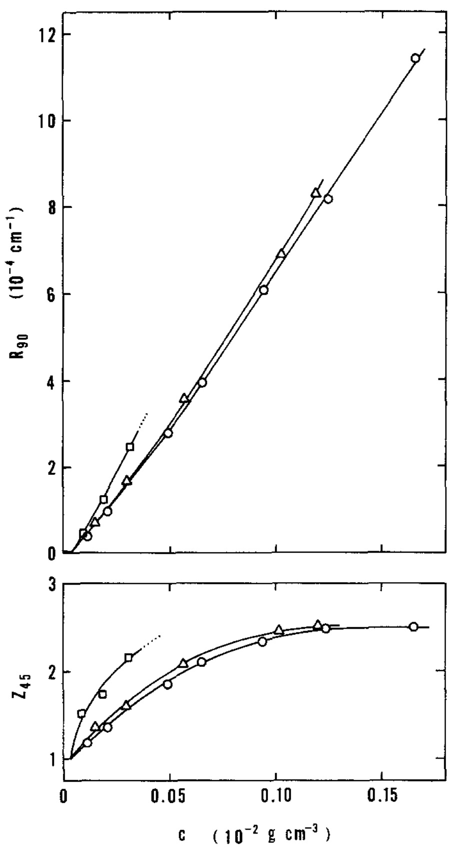

Fig. 1. Reduced scattering intensity in the 90 ° direction (upper) and angular dissymmetry at 45 ° (lower) of scattered light for 0.05 M NaCl solutions at a given HCl concentration. HCl concentration (N): ○ = 0; △ = 10^{-4}; □ = 10^{-3}. The solutions undergo phase separation in dotted parts

Dilute surfactant solutions of higher HCl concentrations developed opalescence which portends successive emulsification or liquid-liquid phase separation. While the dissymmetry reaches a constant value after the gradual initial increase above the critical micelle concentration (CMC), the reduced intensity increases with increasing surfactant concentration beyond the CMC. The values of CMC are listed in table 1. The reduced intensity and the dissymmetry of solutions in the presence of 0.05 M NaCl increase with the addition of HCl, suggesting the increase in size of micelles.

If the effect of external interference is negligibly small, the reciprocal intensity of light scattered in the θ direction from a dilute micellar solution can be expressed by the Debye equation

$$\frac{K(c-c_o)}{R_\theta - R_\theta^o} = \frac{1}{M_w P(\theta)} + 2B(c-c_o) \tag{1}$$

Table 1. Properties of rodlike micelles of dimethyloleylamine oxide in aqueous solutions with high NaCl concentrations

C_A (N)	C_s (M)	$(\partial \tilde{n}/\partial c)_{C_A, C_s}$ ($cm^3 g^{-1}$)	c_o ($10^{-2} g cm^{-3}$)	M_w (10^4)	m_w	$(\overline{R_G^2})_{ls}^{1/2}$ (nm)	$2B$ ($10^{-3} cm^3 g^{-1}$)	pH
0	0.01	0.161_5	0.003	476	15,300	112	~0	7.1-7.2
	0.05	0.161	0.003	690	22,100	127	~0	7.3-7.4
10^{-4}	0.01	0.161_5	0.004	500	16,000	112	0.07	6.8-6.9
	0.05	0.161	0.004	758	24,300	141	~0	7.0-7.1
10^{-3}	0.01	0.167	0.004_5	1,800	58,000	210	0.258	4.8-5.1
	0.05	0.167	0.004	—	—	—	—	—

where R_θ is the reduced intensity at a surfactant concentration, c (g cm^{-3}), and R_θ^o is that at the CMC, c_o. M_w means the weight average molecular weight of micelles, $P(\theta)$ the particle scattering factor, and B the second virial coefficient. The optical constant, K, is given by

$$K = \frac{2\pi^2 \tilde{n}_o^2 (\partial \tilde{n}/\partial c)_{C_A, C_s}^2}{N_A \lambda^4} \qquad (2)$$

where $\tilde{n}_o$ is the refractive index of solvent, and $(\partial \tilde{n}/\partial c)_{C_A, C_s}$ is the specific refractive index increment of solution at constant HCl and NaCl concentrations, C_A (N) and C_s (M). N_A is the Avogadro number, and λ is the wavelength of light in vacuo. For low scattering angles, the particle scattering factor reduces to

$$\left(\frac{1}{P(\theta)}\right)_{\mu:\text{small}} = 1 + \frac{1}{3}\mu^2 (\overline{R_G^2})_{ls} \qquad (3)$$

with

$$\mu = \frac{4\pi \tilde{n}_o}{\lambda} \sin\left(\frac{\theta}{2}\right) \qquad (4)$$

irrespective of particle shape, where $(\overline{R_G^2})_{ls}$ is the light scattering average mean-square radius of gyration of micelles [6–8]. Using the observed values of specific refractive index increment listed in table 1, we can calculate the values of the optical constant and draw the Zimm plot for each micellar solution.

Figure 2 illustrates the Zimm plot for solutions in 0.05 M NaCl with various HCl concentrations. The reciprocal angular envelope of light scattering increases linearly at low scattering angles and convex upward at high scattering angles. When it is extrapolated to zero scattering angle where the value of P (θ) is equal to unity, the reciprocal values of apparent molecular weight at each micelle concentration can be obtained, and they are given in figure 3 (a) as a function of micelle concentration. The values of radius of gyration of micelles, which are obtained from the initial

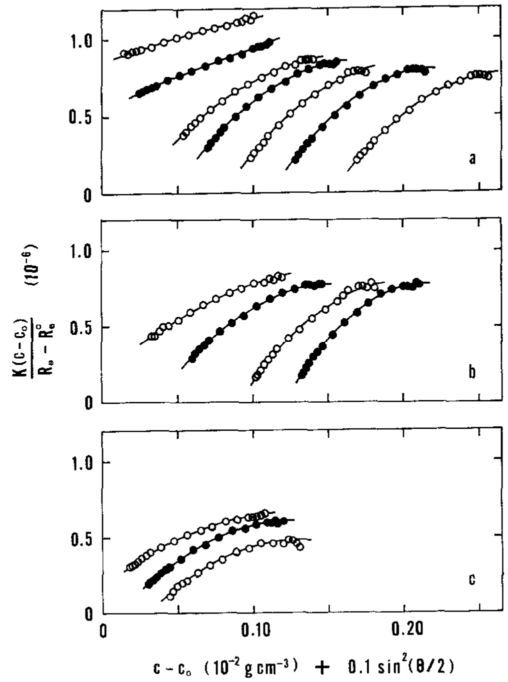

Fig. 2. Zimm plots of light scattering for 0.05 M NaCl solutions at a given HCl concentration. HCl concentration (N): a = 0; b = 10^{-4}; c = 10^{-3}. Micelle concentration (10^{-2} g cm^{-3}), from left to right: a = 0.008, 0.018, 0.047, 0.063, 0.092, 0.121, 0.163; b = 0.026, 0.053, 0.098, 0.129; c = 0.015, 0.027, 0.038

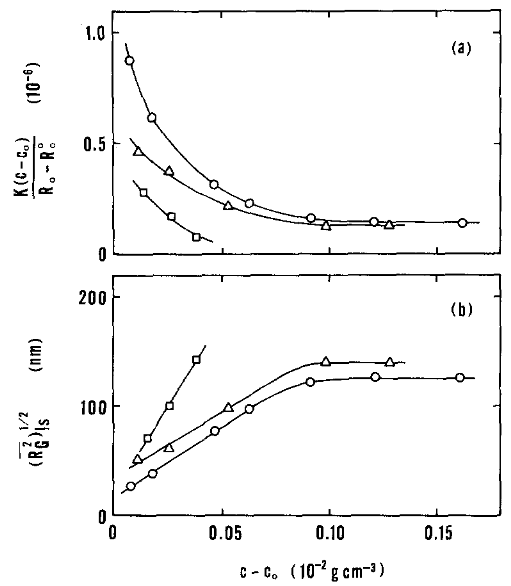

Fig. 3. (a) Debye plots for light scattering in the 0 ° direction and (b) the radius of gyration as a function of micelle concentration. Symbols as given in figure 1

slope at small scattering angles of the Zimm plot, are given in figure 3 (b). Values of apparent molecular weight and radius of gyration gradually increase with increasing micelle concentration and then become constant at high micelle concentrations. This feature indicates that the equilibirum between two kinds of micelles exists; it shifts from the side of small spherical micelles to that of large rodlike micelles, as the micelle concentration increases.

The second virial coefficient for aqueous 0.05 M NaCl solutions of micelles would be negligibly small, as will be discussed later. Then, the Debye plot at zero scattering angle such as that shown in figure 3 (a) can be identified with the reciprocal of the weight-average molecular weight of micelles at each micelle concentration. The constant value of the Debye plot obtained at micelle concentrations higher than 0.1×10^{-2} g cm^{-3}, which is 20–30 times of the CMC, is essentially equal to the reciprocal of molecular weight of the rodlike micelles. Similarly, the constant value of the radius of gyration attained at high micelle concentrations such as those shown in figure 3 (b) can also be assigned to that of rodlike micelles. These values are listed in table 1, together with the values of the weight-average micelle aggregation number, $m_w = M_w/311.6$, and the pH values of corresponding solutions.

The same procedure to obtain the values of the molecular weight and radius of gyration for the rodlike micelles may be applied to the data of light scattering for 0.01 M NaCl solutions in the presence of HCl. In this case, however, the effects of the second virial coefficient are significant, thus giving minima on the Debye plots at zero scattering angle. The values of the second virial coefficient for rodlike micelles can be obtained from the slope at higher micelle concentrations of the Debye plot at zero scattering angle. They are shown in table 1. After having corrected the contribution of the second virial coefficient, we can obtain the values of molecular weight for rodlike micelles as listed in table 1. As seen from this table, both values of aggregation number and radius of gyration of rodlike micelles increase not only with the addition of NaCl but also with the addition of HCl up to 10^{-3} N or with the decrease of pH down to 5.

Flexibility of rodlike micelles

The values of the inverse particle scattering factor at high micelle concentrations, where the contribution of spherical micelles would be negligible, can be evaluated by using equation (1) and the observed values of related parameters. Figure 4 gives the inverse particle scattering factor plotted against $\mu^2\,\overline{(R_G^2)}_{ls}$. The calculated curves for rigid rods [9, 10] and wormlike chains [11] are also drawn in figure 4. The observed values of the inverse scattering factor for rodlike micelles in concentrated NaCl solutions deviate upward from the calculated curve for rigid rods. Thus, rodlike micelles must have some flexibility, which is especially marked for micelles in the NaCl solutions in the presence of 10^{-3} N HCl.

Such a flexible rodlike micelle can be treated as a wormlike chain of Kratky and Porod [12]. If L_c and a represent the contour length and persistence length of a wormlike chain, respectively, its mean-square radius of gyration, $\langle s^2\rangle_o$, and mean-square end-to-end distance $\langle r^2\rangle_o$, are given by [7, 12]

$$\frac{\langle s^2\rangle_o}{a^2} = \frac{L_c}{3a} - 1 + \frac{2a}{L_c}\left[1 - \frac{a}{L_c}\left(1 - e^{-L_c/a}\right)\right] \quad (5)$$

$$\frac{\langle r^2\rangle_o}{2a^2} = \frac{L_c}{a} - 1 + e^{-L_c/a} \quad (6)$$

where the suffix, o, means that the parameters stand for the unperturbed chains without the excluded volume effect. The contour length, L_c, is related to the molecular weight, M, by

$$L_c = M/M_L \quad (7)$$

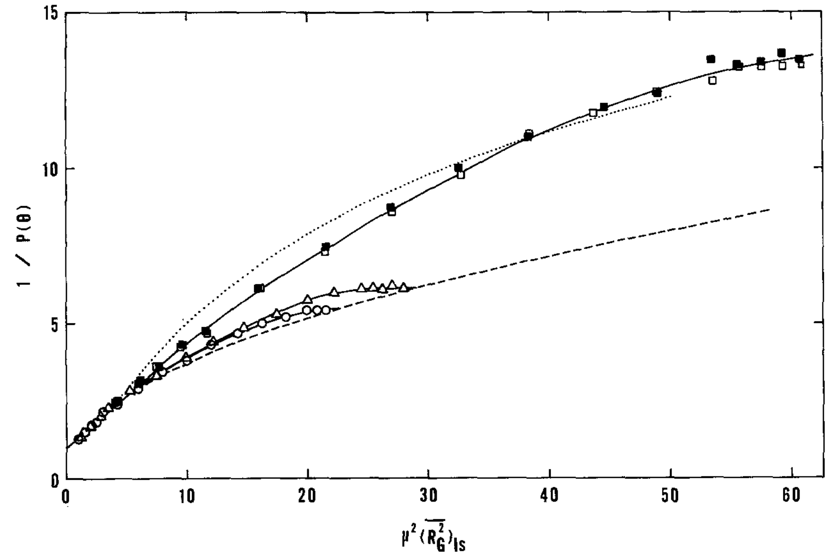

Fig. 4. Inverse particle scattering factor of light scattering as a function of $\mu^2 \overline{(R_G^2)}_{ls}$. Solvent and micelle concentration (10^{-2} g cm^{-3}): ○ = 0.05 M NaCl, 0.121; △ = 10^{-4} N HCl-0.05 M NaCl, 0.129; □ and ■ = 10^{-3} N HCl-0.01 M NaCl, 0.121 and 0.132, respectively. — — — = calculated for rigid rods; ··· = calculated for wormlike chains at $L_c/2a = 5$

where M_L is the molecular weight per unit length. The symbols, $\langle s^2 \rangle_o$ and M, are used as the counterparts corresponding to $\overline{(R_G^2)}_{ls}$ and M_w, respectively, for a monodisperse rodlike micelle. The monodispersity of rodlike micelles has been established both experimentally [2] and theoretically [13].

The value of the molecular weight per unit chain length of 12,000 nm^{-1}, which was obtained in the previous paper [2], can be used for the parameter, M_L. Values of L_c, a, and $\langle r^2 \rangle_o^{1/2}$ evaluated from equations (5)–(7) are listed in table 2. The persistence length of rodlike micelles is smaller for 0.05 M NaCl solutions than for 0.01 M NaCl solutions and decreases with the addition of HCl. The end-to-end distance remains insensitive to the changes in both HCl and NaCl concentrations.

The number of Kuhn's segments, $L_c/2a$, for rodlike micelles, which is a measure of flexibility, is also included in table 2. The estimation of flexibility can be made also from the curves of the inverse particle scattering factor as a function of μ^2 $\overline{(R_G^2)}_{ls}$ as shown in figure 4. The curves observed for rodlike micelles were compared with the theoretical curves for wormlike chains drawn by Sharp and Bloomfield [11], who calculated the $P(\theta)$ curves for various $L_c/2a$ values. The assignable values of $L_c/2a$ are also included in table 2. Although the values from the latter procedure are smaller than those from the former, it can be concluded that the flexibility of rodlike micelles in both 0.01 and 0.05 M NaCl increases with the addition of HCl up to 10^{-3} N. The increased charge makes the rodlike micelles longer and more flexible.

Table 2. Characteristics of rodlike micelles as wormlike chains

C_A (N)	C_s (M)	L_c (nm)	a (nm)	$\langle r^2 \rangle_o^{1/2}$ (nm)	$L_c/2a$	$L_c/2a$[a])
0	0.01	397	1,740	382	0.11	~0
	0.05	575	176	378	1.64	0.5
10^{-4}	0.01	417	560	371	0.37	~0
	0.05	632	203	421	1.56	0.5
10^{-3}	0.01	1,520	107	549	7.10	3.3

[a]) estimated from the curves in figure 4

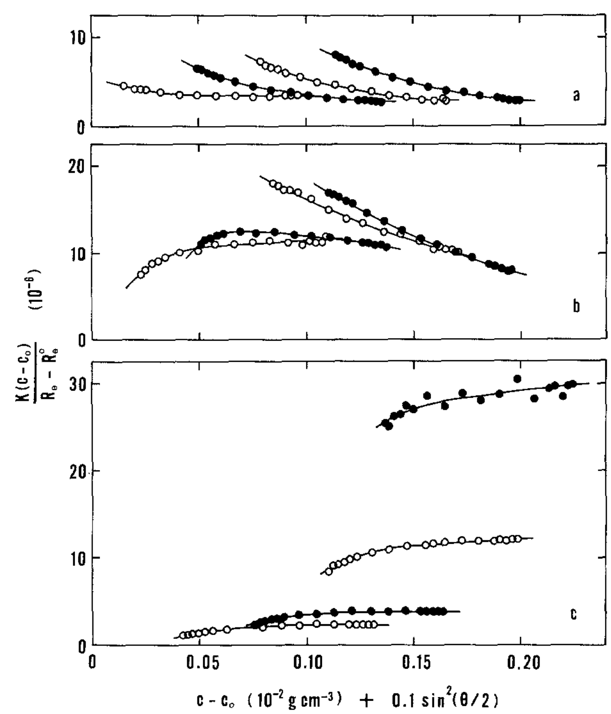

Fig. 5. Zimm plots of light scattering for aqueous solutions at a given HCl concentration. HCl concentration (N): a = 0; b = 10^{-4}; c = 10^{-3}. Micelle concentration (10^{-2} g cm^{-3}), from left to right: a = 0.008, 0.042, 0.072, 0.107; b = 0.016, 0.044, 0.077, 0.103; c = 0.038, 0.072, 0.106, 0.132

Light scattering at zero or low NaCl concentrations

Figure 5 shows the Zimm plots of light scattering for dimethyloleylamine oxide in aqueous HCl solutions without NaCl. The reciprocal angular envelope in pure water decreases with increasing scattering angle. This negative slope results in the angular dissymmetry smaller than unity: light scattering is subject to the effect of external interference [1, 14, 15] due to the long-range intermicellar interaction. The same effect can be found in the angular dependence of light scattering for micelles in 10^{-4} and 10^{-3} N HCl solutions and also in 10^{-3} N HCl-10^{-3} M NaCl solutions. While the Zimm plots for more concentrated micellar solutions in 10^{-4} N HCl have similar features to those in water, the Zimm plots for dilute micellar solutions in 10^{-4} N HCl and for 10^{-3} N HCl solutions of micelles give somewhat different shapes of curves, as seen in figure 5. Micellar solutions in 10^{-3} N HCl-10^{-3} M NaCl show similar features to those in 10^{-3} N HCl, but the values of the reciprocal angular envelope are still low even at high micelle concentrations.

Assuming that the micelles are far apart from one another, so that the effect of external interference may be separated from that of internal interference, then the reduced intensity of light scattered from such a micellar solution is given by [14–18]

$$R_\theta - R_\theta^o = K(c - c_o)\, M_w P(\theta)\, S(\theta)\,. \qquad (8)$$

The structure factor, $S(\theta) \equiv S(\mu)$, arises from the nonrandom arrangement of micelle particles and is related to the radial distribution function, $g(r)$, by

$$g(r) - 1 = \frac{M_w}{2\pi^2 N_A (c - c_o)} \int_0^\infty [S(\theta) - 1] \frac{\sin \mu r}{\mu r} \mu^2 d\mu\,. \qquad (9)$$

The function $g(r)$ denotes the probability of finding a center of mass of another particle at the distance, r, from the center of mass of a specified particle. Since $g(r) = 0$ at small r values, equation (10) is derived.

$$\int_0^\infty [S(\theta) - 1]\mu^2 d\mu = -\,2\pi^2 N_A (c - c_o)/M_w\,. \qquad (10)$$

For the micelles under consideration, the values of $(\overline{R_G^2})_{ls}^{1/2}$ are small, as proved from the later evaluation, so that equation (11) would hold approximately at all scattering angles.

$$P(\theta) = 1 - \frac{1}{3}\mu^2 (\overline{R_G^2})_{ls}\,. \qquad (11)$$

Using the observed values of $(R_\theta - R_\theta^o)/K(c - c_o)$, the two parameters of the micelles, M_w and $(\overline{R_G^2})_{ls}^{1/2}$, can be evaluated from equations (8), (10) and (11). The detailed procedure for the numerical calculation has already been described [1]. The optimum values of the parameters obtained for the rodlike micelles at high micelle concentrations are listed in table 3. The values of weight-average aggregation number and of contour length are also included, together with the concentrations of micellar solution and their pH values. The aggregation number and the radius of gyration of rodlike micelles slightly increase with the addition of HCl in the absence of NaCl.

The data in tables 1 and 3 as well as in the previous work [1,2] lead to the linear relation between $(\overline{R_G^2})_{ls}^{1/2}$ and $M_w^{0.70}$. The power index of 0.70 is closer to 0.6 for random coils in good solvents [19] rather than 1 for rigid rods [8], demonstrating the flexibility of rodlike micelles. It can also be shown that the linear relation of

Table 3. Characteristics for rodlike micelles of dimethyloleylamine oxide in aqueous solutions with zero or low NaCl concentrations

C_A (N)	C_s (M)	$(\partial \tilde{n}/\partial c)_{C_A, C_s}$ ($cm^3 g^{-1}$)	c_o ($10^{-2} g cm^{-3}$)	$c - c_o$ ($10^{-2} g cm^{-3}$)	M_w (10^4)	m_w	$(\overline{R_G^2})_{ls}^{1/2}$ (nm)	L_c (nm)	$2B$ ($10^{-3} cm^3 g^{-1}$)	pH
0	0	0.163	0.004	0.107	89	2,900	25	74	0.92	7.1
10^{-4}	0	0.162	0.004	0.103	83	2,700	39	69	1.05	6.6
10^{-3}	0	0.167	0.004_5	0.132	98	3,100	44	82	0.72	4.5
10^{-3}	10^{-3}	0.167	0.004_5	0.131	149	4,780	42	124	0.40	4.7

log M_w vs. log $(C_o + C_s)$ with a slope 0.31 holds for all micelles, irrespective of different HCl concentrations, expect for the 0.01 M NaCl solution with 10^{-3} N HCl.

Intermicellar interaction

When the solution is dilute, equation (8) can be written as [14,20]

$$\frac{K(c-c_o)}{R_\theta - R_\theta^o} = \frac{1}{M_w P(\theta)} + 2B\,Q(\theta)\,(c-c_o) \qquad (12)$$

where

$$2B = -\frac{N_A}{M_w^2}\int_0^\infty [g(r)-1]\,4\pi r^2 dr = \frac{1-S(0)}{M_w(c-c_o)} \qquad (13)$$

and

$$Q(\theta) = \frac{[1-S(\theta)]}{P(\theta)[1-S(0)]} \qquad (14)$$

where $S(0)$ is the value of the structure factor extrapolated to zero scattering angle.

Equation (12) is identical with equation (1) at low scattering angles, where $P(\theta)$ and $Q(\theta)$ approach unity. Equation (13) allows us to calculate the second virial coefficient by extrapolating values of the structure factor to zero scattering angle.

Values of the second virial coefficient calculated for solutions at higher micelle concentrations are shown in table 3. It is seen that the second virial coefficients $2B$ calculated by equation (13) are almost equal, independent of the micelle concentrations higher than 0.1 × 10^{-2} g cm^{-3}. From this fact, it is expected that values of the second virial coefficient in table 1 calculated from the slope of the reciprocal scattering intensity in the region of high micelle concentrations are reasonable. It is seen from tables 1 and 3 that the second virial coefficient decreases with the addition of NaCl and is zero at high NaCl concentrations. This behavior is not very marked in micellar solutions in the presence of HCl. Although the excluded volume can be easily decreased by the addition of a small amount of salt, the electrostatic effect cannot be shielded sufficiently unless a sufficient amount of salt is added.

The radial distribution function, $g(r)$, represents the mutual arrangement of the micelle particles in solution, and it varies with intermicellar distance, r, as shown in figure 6 for solutions of high micelle concentrations. A small maximum on the $g(r)$ curve for rodlike micelles can be seen at an intermicellar distance of 140–165 nm. The curves do not change significantly, irrespective of whether an electrolyte is present or not.

The interaction force between the particles is related to the radial distribution function. Approximate equations relating the pair potential with the radial distribution function have been derived for simple liquids [5] and applied for latex suspensions [17,18]. According to the theories, Percus-Yevick (PY) and Hypernetted

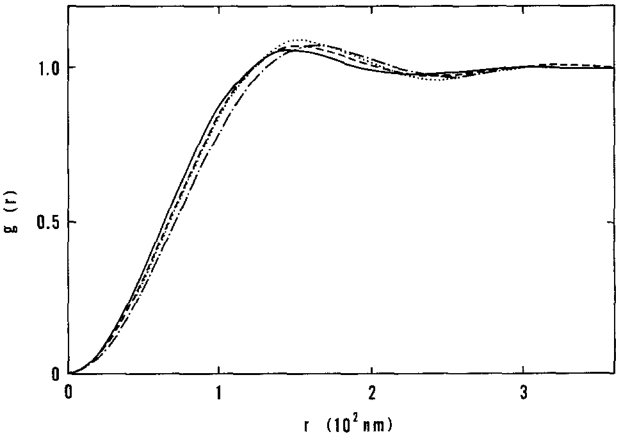

Fig. 6. Plots of the radial distribution function against intermicellar distance. Solvent and micelle concentration (10^{-2} g cm^{-3}): —— = water, 0.107; – – – – = 10^{-4} N HCl, 0.103; ···· = 10^{-3} N HCl, 0.132; –·–·– = 10^{-3} N HCl–10^{-3} M NaCl, 0.131

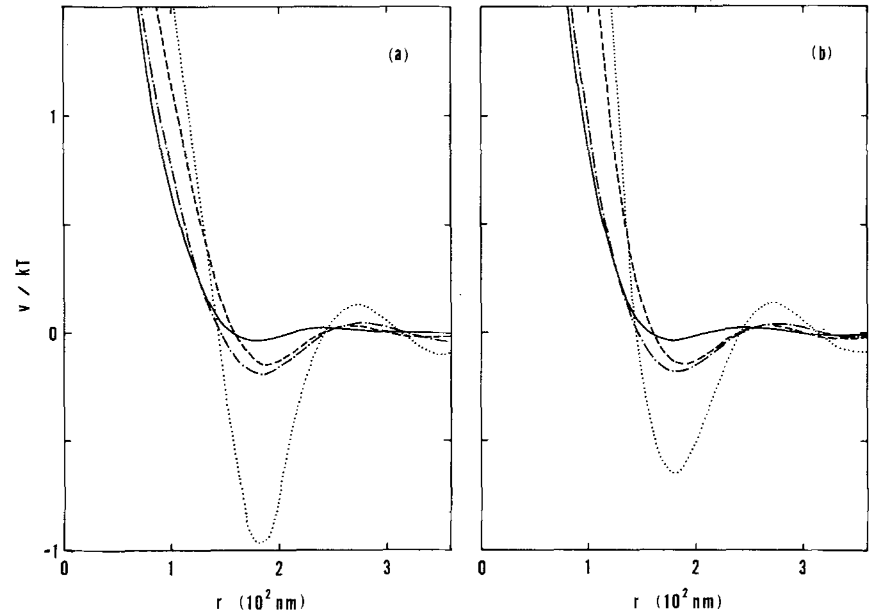

Fig. 7. Intermicellar pair potential as a function of intermicellar distance. (a) PY approximation; (b) HNC approximation. Legends of curves correspond to the same solvent and micelle concentration as in figure 6

Chain (HNC), which have been most popular, the interparticle pair potential, $v(r)$, can be derived by

$$\frac{v_{\mathrm{PY}}(r)}{kT} = \ln\left[1 - \frac{c(r)}{g(r)}\right] \tag{15}$$

and

$$\frac{v_{\mathrm{HNC}}(r)}{kT} = g(r) - 1 - c(r) - \ln[g(r)] \tag{16}$$

respectively, where k is the Boltzmann constant and T is the temperature. The direct correlation function, $c(r)$, is given by

$$c(r) = \frac{M_w}{2\pi^2 N_A (c - c_o)} \int_0^\infty \frac{[S(\theta) - 1]}{S(\theta)} \frac{\sin \mu r}{\mu r} \mu^2 d\mu . \tag{17}$$

If all the interactions between micelles are assumed to arise from their centers of mass which are separated by the distance, r, then equations (15) and (16) may be applied to the micellar solution. The intermicellar pair potential calculated by equations (15) or (16) through equations (9) and (17) is shown in figure 7 in several conditions.

The pair potentials between rodlike micelles obtained by the PY and HNC equations are very similar, except for slight deviation from each other at short intermicellar distances. The steep increase of the pair potential at short distances is due to the strong repulsive interaction between micelles, and it is stronger in the addition of HCl and weaker in the addition of NaCl. For nonionic micelles the steric repulsion is dominant at short distances, and for ionic micelles the electrostatic effect is superposed to the steric repulsion. The long-range electrostatic repulsion should increase with the addition of HCl and is depressed by the addition of NaCl. Each pair potential reveals a minimum at an intermicellar distance around 180 nm, which becomes deeper with the addition of HCl but shallower with the addition of NaCl.

The variation of the dissymmetry with micelle concentration is obtained from equations (8) and (9). If the Fourier transform of equation (9) is taken and $\sin \mu r$ is expanded against μr, omitting higher terms, the structure factor is rewritten as

$$S(\theta) \approx 1 - 2B(c - c_o) M_w \left\{1 - \frac{\mu^2}{6} \frac{\int_0^\infty [g(r) - 1] 4\pi r^4 dr}{\int_0^\infty [g(r) - 1] 4\pi r^2 dr}\right\} . \tag{18}$$

Introducing equation (18) into $S(\theta)/S(\pi-\theta)$, expanding the denominator for small values of $c - c_o$, and again omitting higher terms, we have

$$\frac{S(\theta)}{S(\pi-\theta)} \approx 1 + \frac{1}{6} N_A (c - c_o) \left(\frac{4\pi \tilde{n}_o}{\lambda}\right)^2 (\cos\theta) \int_0^\infty [g(r) - 1] 4\pi r^4 dr. \tag{19}$$

Now it is assumed that the radial distribution function has a property such as $g(r) = 0$ for $0 < r \le R$ and $g(r) = 1$ for $r \ge R$, where R is the intermicellar distance of the closest approach. This assumption is derived from the feature of the radial distribution function as shown in figure 6. Then by means of equation (8), the dissymmetry is expressed by

$$z_\theta \approx [z_\theta] \left\{1 - \frac{(4\pi)^3 \tilde{n}_o^2 N_A R^5}{30 \lambda^2} (\cos\theta)(c - c_o)\right\} \tag{20}$$

where $[z_\theta]$ is the intrinsic dissymmetry for the rodlike micelles. It is noted that $\cos\theta$ is positive.

If the effect of external interference is more dominant than that of internal interference, the value of dissymmetry, z_θ, should monotonically decrease from that of the intrinsic dissymmetry, $[z_\theta]$, as the micelle concentration increases. This is the case observed for solutions of dimethyloleylamine oxide with zero or low NaCl concentrations. Specifically, when external interference is superior to internal interference, the dissymmetry may be less than unity, as is apparent for micelles in water and in 10^{-4} N HCl.

Discussion

Our previous work on light scattering from micellar solutions of dimethyldodecylamine oxide produced the following results [21]. Molecules of dimethyldodecylamine oxide are nonionic or only very weakly cationic in aqueous solution. They are protonated in the presence of HCl. In aqueous solutions without NaCl, charged micelles of dimethyldodecylamine oxide should decrease their aggregation number with increasing the degree of protonation. This can be ascribed to the electrostatic repulsion between surfactant micelles. In the presence of NaCl, however, spherical micelles associate together into large micelles at half-protonation of molecules.

In contrast to dimethyldodecylamine oxide, dimethyloleylamine oxide can form rodlike micelles even in pure water, having molecular weight as large as 10^6. In the absence of added NaCl, the micelle molecular weight of dimethyloleylamine oxide in aqueous solutions slightly increases by the addition of HCl up to 10^{-3} N. This HCl concentration lowers pH to 4.5, leading to the formation of half-protonated rodlike micelles. Nevertheless, in concentrated NaCl solutions, the aggregation number of rodlike micelles markedly increases by the addition of 10^{-3} N HCl. The amine oxide is subject to the strong salting-out effect by added NaCl, and its molecules are dehydrated and tend to form larger micelles [21]. The addition of HCl up to almost half-protonation might cause further dehydration of molecules in rodlike micelles and, moreover, promote hydrogen bonding between protonated and nonprotonated molecules in a micelle.

The flexibility of rodlike micelles of dimethyloleylamine oxide also increases with the addition of NaCl an HCl. As suggested for the reason of the flexibility of rodlike micelles of hexaoxyethylene cetyl ether [22], the hydration of the amine oxide group which is strongly hydrophilic may confer some rigidity on rodlike micelles. As the addition of NaCl would promote the dehydration, the addition of HCl may also affect the dehydration of molecules or micelles of dimethyloleylamine oxide by the binding of counterions, besides the protonation of amine oxide to form N-hydroxyammonium ion. In these ways, the rodlike micelles acquire the flexibility and tend to bend themselves.

The second virial coefficients for aqueous solutions of nonionic surfactants such as polyoxyethylene alkyl ether [23] are of the order of 10^{-4} cm^3 g^{-1}. Spherical micelles of ionic surfactants give the second virial coefficients of the order of 10^{-3} cm^3 g^{-1} in 0.01 and 0.05 M NaCl [24–26], and these values are reduced by further addition of NaCl. The second virial coefficient for a dimethyloleylamine oxide solution in pure water has a value of the same order as those for polyoxyethylene series [23]. Even in the presence of HCl, the second virial coefficients of dimethyloleylamine oxide are still lower than those for ionic surfactants as well as for fully protonated dimethyldodecylamine oxide in solution [21]. However, the large value of micelle molecular weight in 10^{-3} N HCl and 0.01 M NaCl solution is strongly compensated by the effect of the value of the second virial coefficient, as seen in table 1.

As can be seen from figure 7, the intermicellar pair potential of rodlike micelles of dimethyloleylamine oxide gives the following changes by the addition of

HCl and NaCl. The depth of the potential well amounts to 1.0–0.7 kT or 600–400 cal mole^{-1} in the presence of 10^{-3} N HCl, but the addition of 10^{-3} M NaCl reduces it to the value comparable with those for the nonionics. That is, the addition of HCl makes the attraction between two micelles stronger, and further addition of NaCl makes this attraction weaker. This situation is somewhat similar to that observed for aqueous solutions of charged monodisperse polystyrene latices in water and in the presence of added salt [27, 28], although the mechanism for the nonrandom arrangement of solute particles would differ between hard sphere particles and rodlike micelles.

The observed behavior of pair potential for the charged rodlike micelles may be tentatively explained by the change in aggregation number. The rodlike micelles in 10^{-3} N HCl should be swollen by intramicellar electrostatic repulsion, and the combination of the steric and electrostatic repulsion with the long-range van der Waals attraction between two large micelles forms a deep potential well at a distance around 180 nm. By the addition of 10^{-3} M NaCl, the electrostatic repulsion is reduced, so that the rodlike micelles grow larger, and the steric repulsion potential shifts towards larger distances; thus the potential well at 180 nm becomes shallower.

Recently, intermicellar interaction of surfactants in aqueous solutions has been investigated by many workers [29–36]. Dynamic light scattering of ionic micelles in aqueous solutions was measured and the results were analyzed on the basis of the DLVO theory [29, 30]. Small angle neutron scattering was measured on aqueous solutions of lithium dodecyl sulfate and gave the intermicellar structure factor from the intensity distribution [31, 32]. All these micelles are supposed to be spherical, but no attempts to derive intermicellar potentials have been made.

Small angle neutron scattering from aqueous solutions of some ionic surfactants having bulky and specific counterions was observed and showed evidence for the formation of rodlike micelles in water, together with the existence of neighboring orders arising from intermicellar interaction [37, 38]. They are tetramethylammonium perfluorooctane sulfonate [37] and cetylpyridinium salicylate [38].

Static light scattering measurements on polymethyl methacrylate latices in benzene [18, 39] and charged polystyrene latices in aqueous solutions of low NaCl concentrations [17, 40] showed strong external interference, leading to the significant structure factors. Similar phenomena on nonrandom arrangements of macromolecules were observed for globular proteins [41] and polyelectrolytes [14, 42] in the absence of added salt by means of light scattering.

Acknowledgement

We are grateful to Drs. Kenichi Hattori and Fumio Hoshino for kindly providing us with the valuable sample.

References

1. Imae T, Ikeda S (1984) J Coll Interf Sci 98:363
2. Imae T, Ikeda S (1984) Coll & Polym Sci 262:497
3. Imae T, Kamiya R, Ikeda S (1984) J Coll Interf Sci 99:300
4. Zernike F, Prins JA (1927) Z Physik 41:184
5. Hansen JP, McDonald IR (1979) Theory of Simple Liquids, Academic Press, London
6. Zimm BH (1948) J Chem Phys 16:1099
7. Benoit H, Doty P (1953) J Phys Chem 57:958
8. Geiduschek EP, Holtzer A (1958) Advan Biol Med Phys 6:431
9. Debye P, Anacker EW (1950) J Phys Colloid Chem 55:644
10. Doty P, Steiner RF (1950) J Chem Phys 18:1211
11. Sharp P, Bloomfield VA (1968) Biopolymers 6:1201
12. Kratky O, Porod G (1949) Rec Trav Chim 68:1106
13. Ikeda S (1984) J Phys Chem 88:2144
14. Ehrlich G, Doty P (1954) J Amer Chem Soc 76:3764
15. Burchard W (1969) Polymer 10:29
16. Brown JD, Pusey PN, Goodwin JW, Ottewill RH (1975) J Phys A: Math Gen 8:664
17. Schaefer D (1977) J Chem Phys 66:3980
18. Nieuwenhuis EA, Vrij A (1979) J Coll Interf Sci 72:321
19. de Gennes PG (1979) Scaling Concepts in Polymer Physics, Cornell Univ Press, Ithaca–London
20. Albrecht AC (1957) J Chem Phys 27:1014
21. Ikeda S, Tsunoda M, Maeda H (1979) J Coll Interf Sci 70:448
22. Elworthy PH, Macfarlane CB (1963) J Chem Soc 907
23. Schick MJ, Atlas SM, Eirich FR (1962) J Phys Chem 66:1326
24. Ikeda S, Ozeki S, Tsunoda M (1980) J Coll Interf Sci 73:27
25. Hayashi S, Ikeda S (1980) J Phys Chem 84:744
26. Ozeki S, Ikeda S (1984) Coll & Polym Sci 262:409
27. Hachisu S, Kobayashi Y, Kose A (1973) J Coll Interf Sci 42:342
28. Ottewill RH (1980) Prog Coll & Polym Sci 67:71
29. Cheng DCH, Gulari E (1982) J Coll Interf Sci 90:410
30. Dorshow RB, Bunton CA, Nicoli DF (1983) J Phys Chem 87:1409
31. Bendedouch D, Chen SH (1983) J Phys Chem 87:1653
32. Bendedouch D, Chen SH, Koehler WC (1983) J Phys Chem 87:2621
33. Hayter JB, Zulauf M (1982) Coll & Polym Sci 260:1023
34. Hayter JB, Penfold J (1983) Coll & Polym Sci 261:1023
35. Triolo R, Magid LJ, Johnson Jr JS, Child HR (1982) J Phys Chem 86:3689
36. Magid LJ, Daus KA, Butler PD, Quincy RB (1983) J Phys Chem 87:5472
37. Hoffmann H, Kalus J, Reizlein K, Ulbricht W, Ibel K (1982) Coll & Polym Sci 260:435
38. Kalus J, Hoffmann H, Reizlein K, Ulbricht W, Ibel K (1982) Ber Bunsenges Phys Chem 86:37
39. Nieuwenhuis EA, Pathmamanoharan C, Vrij A (1981) J Coll Interf Sci 81:196
40. Ottewill RH, Richardson RA (1982) Coll & Polym Sci 260:708

41. Doty P, Steiner RF (1952) J Chem Phys 20:85
42. Oth G, Doty P (1952) J Phys Chem 56:43

Received October 25, 1984;
accepted January 28, 1985

Authors' address:

Toyoko Imae and Shoichi Ikeda
Department of Chemistry
Faculty of Science
Nagoya University
Chikusa, Nagoya 464, Japan